16th World Conference on Earthquake, 16WCEE 2017

Santiago Chile, January 9th to 13th 2017

Paper N° 147

Registration Code: S-M1462884689

EARTHQUAKE POTENTIAL AND MAGNITUDE LIMITS IN SOUTHERN EUROPE

Y. Rong[(1)], P. Bird[(2)], D. D. Jackson[(3)]

[(1)]*Senior Lead Research Scientist, Center for Property Risk Solutions, FM Global, Research Division, Norwood, Massachusetts, USA, yufang.rong@fmglobal.com*

[(2)]*Professor Emeritus, Department of Earth, Planetary, and Space Sciences, University of California, Los Angeles, California, USA, pbird@epss.ucla.edu*

[(3)]*Professor Emeritus, Department of Earth, Planetary, and Space Sciences, University of California, Los Angeles, California, USA, djackson@g.ucla.edu*

Abstract

Seismic Hazard Harmonization in Europe (SHARE) published new seismic hazard maps of Europe in 2013. Seismic source models are the basis for hazard calculations. SHARE constructed three seismic source models based on historical earthquakes and geological fault data. The SHARE source models provided parameters from which magnitude-frequency distributions can be specified for each of 437 seismic source zones covering most of Europe. To evaluate the SHARE seismic source models, we construct an earthquake potential model of Southern Europe using the Global Strain Rate Map released in 2014. Because the individual SHARE area source zones are too small to have sufficient data for accurate estimates, we combine the source zones into five groups according to SHARE's estimates of maximum magnitude. Using the strain rates, we calculate tectonic moment rates for each group. Then, we infer seismicity rates and probable maximum earthquake magnitudes from the tectonic moment rates. For two groups, the tectonic moment rates are higher than SHARE seismic moment rates; SHARE rates of large earthquakes are lower than those inferred from tectonic moment rates, but higher than those based on historical earthquakes. For another group, the tectonic moment rate is lower than SHARE seismic moment rates; SHARE rates of large earthquakes are higher than those inferred from tectonic moment rate, but lower than what historical data show. For the other two groups, the seismicity rates from tectonic moment rate, historical data, and SHARE models are consistent. For four groups, the maximum magnitudes used by SHARE are fairly consistent with the probable maximum magnitudes inferred from tectonic strain rates. This study demonstrates that: 1) the strain rate data are useful for constraining seismicity rates and magnitude limits; and 2) the SHARE seismic source models fit for the purpose.

Keywords: strain rate; tectonic moment; magnitude-frequency distribution; maximum probable earthquake magnitude.

1. Introduction

Seismic Hazard Harmonization in Europe (SHARE), funded by the European Commission, released a community-based probabilistic seismic hazard model in 2013 [1, 2]. The SHARE project compiled homogeneous and harmonized databases, used updated ground motion models, and extended the study region to cover all of Europe. The SHARE seismic hazard model represents a huge improvement over the previous models [3].

Seismic source models quantify earthquake magnitudes and rates at each location. They are the foundation for building a seismic hazard model. SHARE developed three seismic source models [2]: the area source zone model, which assumes a homogeneous distribution of earthquake activity within each source zone; the SEIFA model, which is a zoneless model that distributes earthquake activity rates in space based on a combination of smoothed earthquake density and accumulated moment on faults; and the fault source model, which infers future seismic activity from estimated slip rates on active faults. The final seismic hazard maps were produced by weighting the hazards calculated using each of the three seismic source models. The three seismic source models are based mainly on historical earthquakes and seismogenic fault data.

Other useful information for modeling seismic activity are geodetic measurements. Geodetic strain rate, which is usually derived from geodetic GPS measurements, can represent a useful approximation of long-term tectonic deformation. The Global Earthquake Model (GEM) Foundation released the latest Global Strain Rate Model (GSRM v2.1) in 2014 [4, 5]. The deformation of the Euro-Mediterranean region is reflected in a wide collision and subduction zone in southern Europe caused by the interaction between the Eurasia and Africa plates. GSRM v2.1 described the deformation by gridded interseismic strain rate tensors. In this study, we calculate tectonic moment rates for southern Europe using GSRM v2.1. We then derive seismicity rates and maximum probable magnitudes based on tectonic moment rates. We compare the seismicity rates and maximum probable magnitudes derived from the strain rate model with those of the SHARE seismic source zone models. The study serves as an independent evaluation of the SHARE seismic source zone models.

2. Data

2.1 Historical earthquake catalogs

A historical earthquake catalog is an important input for modeling seismic activity. In the framework of the SHARE project, three historical earthquake catalogs were compiled: the SHARE European Earthquake Catalog for the years 1000 to 1899 (SHEEC 1000-1899); SHEEC 1900-2006; and the SHARE earthquake catalog for Central and Eastern Turkey (SHARE-CET). SHEEC 1000-1899 contains 4722 historical earthquakes [6]. SHEEC 1900-2006 [7] consists of over 13,600 events. Both catalogs cover the territories belonging to the European Union member states and neighboring areas out to 32°E. The SHEEC 1900-2006 is based on the European-Mediterranean Earthquake Catalogue [8] with modifications. The SHARE-CET catalog was compiled to complement the two SHEECs [9]. The SHARE-CET catalog covers the Turkish territory and Cyprus from 32° E to 45° E. It includes 6,170 events from 1000 A.D. to 2006. All three SHARE catalogs express earthquake magnitudes by moment magnitude (m_w). We use the SHARE historical catalogs (Fig.1) for the analysis in this paper.

2.2 Global strain rate model (GSRM) v2.1

To construct GSRM v2.1, Kreemer *et al.* [4, 5] computed 22,511 interseismic GPS velocities, including 6,739 from continuous-GPS sites. Among them, 17,663 velocities are in the deforming zones, and 4,848 are on rigid plates. The model consists of a grid of 145,086 deforming cells of 0.2° by 0.25° size and 50 large rigid plates or blocks. To determine a priori which cells should be allowed to deform and which not, the authors followed the plate definitions of the plate-tectonic model Plate Boundaries by Bird [10] augmented by the boundary definitions of Chamot-Rooke and Rabaute [11]. GSRM v2.1 includes estimates of uncertainty: GPS velocity uncertainties are typically 0.1 - 0.3 mm/yr, and the strain rate uncertainty at any point is largely dependent on the GPS station density.

The tectonics of southern Europe and the eastern Mediterranean are dominated by the interaction between the Eurasia and Africa plates. The Africa plate is moving northwards into the Eurasia plate, creating subduction zones and crustal fault zones. A broad and complex belt of seismicity and deformation from the Alps in the north to the Aegean subduction zone in the south results in a complicated pattern of crustal stress and strain fields. The oceanic plate boundaries of the Atlantic exhibit simple deformation, characterized by narrow seismic belts. Northern Europe is a relatively stable continental region, where GSRM v2.1 assumes zero strain rate. Therefore, we focus on southern Europe where the tectonics are more active and are described by GSRM v2.1 (Fig.1).

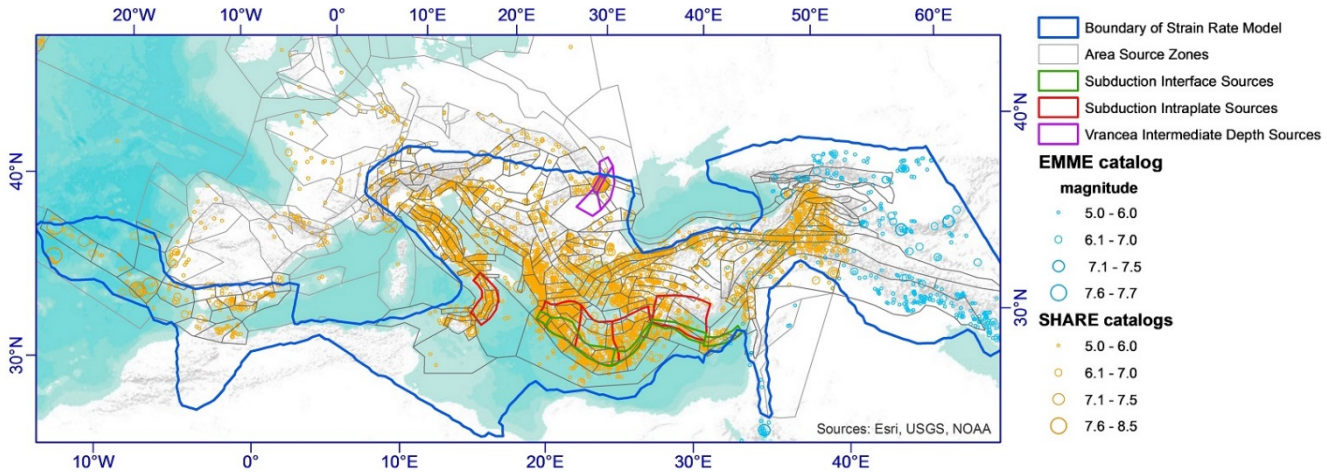

Fig. 1 - SHARE seismic source zones [3] shown by polygons and SHARE (brown circles) and EMME (blue circles) historical earthquake catalogs. The thick blue outline surrounds the study area of this paper, defined by the coverage of the GSRM v2.1 model.

3. Estimating Tectonic Moment from Strain Rate for Southern Europe

The tectonic moment rate can be calculated from the strain rate model based on the reasonable assumption that the long-term average rate of elastic strains is negligible in comparison to the rate of permanent strains accumulated by frictional faulting, cold-work plasticity, solution transfer, dislocation creep, and other mechanisms [12]. The tectonic moment rate of an area A (such as one GSRM v2.1 cell) with uniform long-term permanent strain rate can be estimated by:

$$\dot{M}_T = A\langle cz\rangle\mu \begin{cases} 2\dot{\varepsilon}_3; & \text{if } \dot{\varepsilon}_2 < 0 \\ -2\dot{\varepsilon}_1; & \text{if } \dot{\varepsilon}_2 > 0 \end{cases} \quad (1)$$

where c is the dimensionless seismic coupling (the fraction of frictional sliding that occurs in earthquakes), μ is the elastic shear modulus, z is the potentially seismogenic depth range (depth to the brittle/ductile transition), and brackets $\langle\ \rangle$ indicate a mean value. Bird and Kagan [13] termed the product of c and z the 'coupled thickness of seismogenic lithosphere'. Here, we use the SHIFT-GSRM2 algorithm of Bird and Kreemer [14] to estimate tectonic moment rates.

We calculate the tectonic moment rate for the region covered by the strain rate model to compare with the seismic moment rate inferred from SHARE models. Because we do not intend to compare the tectonic moment rate for each cell of the GSRM v2.1 grid or each SHARE area source zone, we first define four superzones by combining SHARE area source zones (Fig.1) according to their maximum magnitudes (m_{max}) assigned by SHARE [3]. Note that SHARE used a logic tree to capture the uncertainty of m_{max}. For most of the zones, four m_{max} values (m_{max01} to m_{max04}) were assigned to each zone in 0.2 magnitude unit increments. The smallest value (m_{max01}) has the highest weight of 0.5. The three other values usually have the weights of 0.2, 0.2, and 0.1, and the weight 0.1 is given to m_{max04}, the highest m_{max}. According to the m_{max} values of the area source zones, the Aegean subduction zone belongs to superzone 2. However, the subduction zone has different tectonics than other

shallow crustal regions in superzone 2. Thus, we separate superzone 2 into crustal and subduction regions. We number the subduction region superzone 5 (Fig.2). Note that superzone 5 includes both subduction interface and intraplate sources and some crustal area sources to the south of the subduction sources. We intentionally do this to account for the fact that a fraction of subduction zone activity is unilaterally spread in the direction of the outer-rises to approximate plate-bending seismicity in the SHIFT-GSRM2f calculations [14]. Some of the source zones are partially outside the strain-rate model coverage. This will not affect the tectonic moment rate results because the strain rate is zero outside the strain rate modeling area. To distinguish the superzones defined here from those defined by SHARE for other purposes, we call the five superzones defined here 'Groups' (Fig.2).

Because of the complex shape of the area source zones and relatively large cell size of the strain-rate model, we use an algorithm to calculate the tectonic moment rate of each group: each active cell of the strain-rate model is divided into N^2 sub-cells (where N = 1, …, 20), and the quantum of tectonic moment rate associated with each sub-cell is transferred to a Group according to which zone (if any) its center-point falls into. This computation is repeated with 20 values of N to demonstrate convergence.

Uncertainty in the tectonic moment rate has several contributions. The most important one, which we compute, is its dependence on the uncertainties in the mean coupled thicknesses $\langle cz \rangle$ in the ten columns (j = 1, …, 10, corresponding to different types of plate boundary of Table 5 in [13]. The ten fractional uncertainties are asymmetrical because the 95% confidence bounds are asymmetrical [13]. For six values of j, the high-side and low-side uncertainties (each of which is half of the 95% confidence range) are available, and the average ratio of mean-uncertainty/low-side-uncertainty is 2.17. Where only a low-side uncertainty is available, we assume that the mean uncertainty is 2.17 times of the low-side uncertainty. Then, for each of the ten classes, the low-side and high-side uncertainties are averaged for the computation of uncertainty of tectonic moment rate.

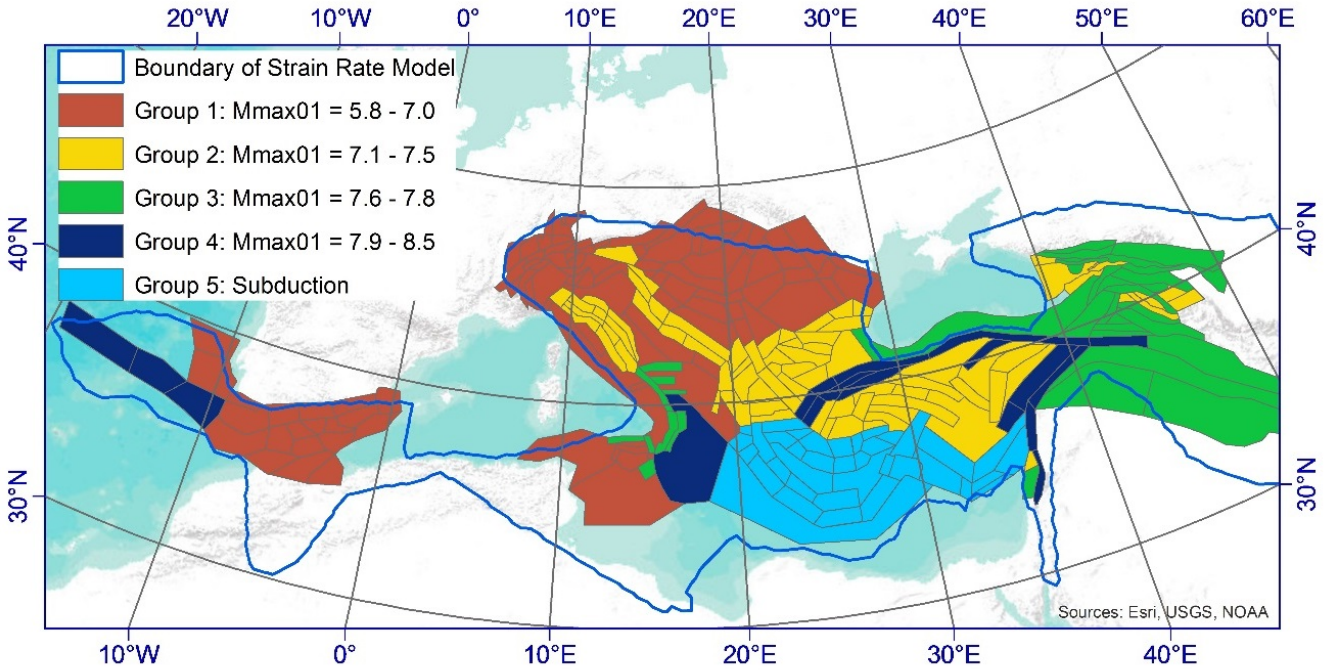

Fig. 2 - Groups in the southern Europe formed by unifying SHARE area source zones by their m_{max} ranges. The value of m_{max01} is used because it has the highest logic tree weight.

These group tectonic moment rates, and their minimum uncertainties, are reported in Table 1. The uncertainties are in the range 30-60% of the moment rates. For comparison, Table 1 also shows the seismic moment rates calculated from the SHARE area source zone ($\dot{M}_{as}$) and SEIFA ($\dot{M}_{sf}$) models. To calculate $\dot{M}_{as}$,

we first calculate the seismic moment rate for each of the SHARE area source zones by using the SHARE Gutenberg-Richter (GR) *a*- and *b*- values and m_{max}. The $\dot{M}_{as}$ values of Groups 1-4 are simply the sum of seismic moment rate of each area source zones that belong to the group. For Group 5, the $\dot{M}_{as}$ value includes the seismic moment rate from both crustal area source zones and the subduction interface zones. For the calculation of $\dot{M}_{sf}$, we simply sum the seismic moment rate of each grid cell of the SEIFA model that falls into the group. The seismic moment rate for a SEIFA grid cell is calculated using the magnitude-frequency distribution for the cell provided in the SHARE model. However, the SEIFA model does not cover the area to the east of 45°E, where Groups 2 and 3 extend. Thus, the comparison with the SEIFA model is only valid for Groups 1, 4, and 5. Table 1 shows that $\dot{M}_{as}$ is less than 20% of $\dot{M}_T$ for Groups 1 and 5, but about 150% of $\dot{M}_T$ for Group 4. $\dot{M}_{sf}$ is about 44% of $\dot{M}_T$ for Group 1 and 14% for Group 5, but about 200% of $\dot{M}_T$ for Group 4.

In SHIFT-GSRM2f [14] and the calculations above, the Aegean subduction zone (Group 5) is considered to have seismic coupling equivalent to the global average of all low-convergence-velocity subduction zones. However, a possible further distinction was raised by [15]: the Aegean subduction zone may have already consumed evaporite sediments laid down in the Mediterranean basin in Messinian time. Thus, its megathrust surface may have even lower seismic coupling (more aseismic slip) than is typical of low-velocity subduction zones. In an extreme model which has the Aegean megathrust surface entirely uncoupled, the earthquake (and seismic moment) production rates of this subduction zone would come entirely from plate-bending earthquakes. Based on Fig.13 of [16], this would suggest that its tectonic moment rate would be only ~38% of the amount computed above. The tectonic moment of this scenario is listed in Table 1 as an alternative for Group 5.

Table 1 – Tectonic and seismic moment rates for the groups

Group	$\dot{M}_T$ (10^{18} N·m/yr)	$\sigma(\dot{M}_T)$ (10^{18} N·m/yr)	$\frac{\sigma(\dot{M}_T)}{\dot{M}_T}$ (%)	$\dot{M}_{as}$ (10^{18} N·m/yr)	$\frac{\dot{M}_{as}}{\dot{M}_T}$ (%)	$\dot{M}_{sf}$ (10^{18} N·m/yr)	$\frac{\dot{M}_{sf}}{\dot{M}_T}$ (%)
1	9.2	3.4	37.6%	1.8	19.7%	4.1	44.2%
2	13.9	4.2	30.2%	12.7	91.4%	9.4[§]	67.9%[§]
3	18.1	9.1	50.0%	10.7	58.8%	11.0[§]	60.8%[§]
4	15.4	5.3	34.1%	23.2	151.1%	30.0	195.1%
5	110.0	66.0	59.9%	15.7	14.2%	15.0	13.6%
5[&]	41.8	25.1	59.9%	15.7	37.6%	15.0	35.9%
Total	166.6	88	52.8%	64.1	38.5%	69.5	22.7%
Total[#]	98.4	47.1	47.9%	64.1	65.1%	69.5	59.8%

[&]The alternative scenario of Group 5, in which the Aegean megathrust surface is considered as entirely uncoupled.

[§]The SEIFA model does not cover the entire area of the Groups 2 and 3. Therefore, the values listed in the table are only for the areas covered by the SEIFA model.

[#]The results by using the alternative scenario of Group 5.

4. Comparing Seismicity Rates Determined from Geodetic Strain Rates with SHARE Models and Historical Data

4.1 Seismicity rates from SHARE models and from historical data

We calculate seismicity rates (magnitude-frequency distributions) for the five groups. The seismicity rate of the SHARE area source zone model is calculated by summing up the rates for each area source that falls into the group. The seismicity rate of the SEIFA model is calculated by summing up the rates for each SEIFA grid cell that falls into the group. Because the SEIFA model does not cover the entire Groups 2 and 3, we estimate the seismicity rate only for Groups 1, 4, and 5 for this model.

We rely on SHARE historical earthquake catalogs to calculate historical seismicity rates. We first perform this calculation for each of the SHARE area source zones. However, the SHARE historical catalogs do not cover the area to the east of 45°E. For the source zones in this area, our calculation is based on the EMME (Earthquake Model of the Middle East Region, http://www.emme-gem.org/) historical catalog. The completeness times of an earthquake catalog are needed for calculating seismicity rate. For the source zones covered by SHARE historical earthquake catalogs, we use the catalog completeness times estimated by the SHARE project [17]. For several areas that are not covered by the SHARE catalogs, we estimate the completeness times of the EMME catalog by plotting the time history of annual and cumulative numbers of earthquakes above each magnitude. The seismicity rates based on SHARE models and historical data are illustrated in Fig.3a to Fig.3f.

4.2 Seismicity rates inferred from tectonic moment rate

We construct earthquake magnitude-frequency distributions using the tectonic moment rate as the total moment rate budget for each of the groups. We assume that the earthquake occurrence rate follows a Tapered Gutenberg-Richter (TGR) distribution. The TGR relation is best expressed in seismic moment, M, instead of magnitude (m_w) [18]:

$$F(M) = \alpha_t \left(\frac{M_t}{M}\right)^{\beta} exp\left(\frac{M_t - M}{M_c}\right) for\ M_t \leq M < \infty \quad (2)$$

where M is in N·m, and $M = 10^{1.5m_w + 9.05}$ [19] .

Here, $F(M)$ is the rate of earthquakes with moment larger than M, and β equals 2/3 of the GR b-value. M_c is called corner moment (the corresponding magnitude is called corner magnitude, m_c), which controls the distribution in the upper range of M. M_t is a threshold moment (the corresponding magnitude is threshold magnitude, m_t) above which the catalog is assumed to be complete, and α_t is the seismicity rate for earthquakes with moment M_t and greater. To construct a TGR magnitude-frequency distribution, three parameters need to be determined: α_t, β, and M_c (or m_c).

For α_t, we adopt the annual earthquake rate estimated from the historical catalogs at $m_t \geq 5.0$. For β, we use 2/3 (asymptotically equivalent to b = 1.0) for all the five groups. The theory of universal b-value has been supported by many studies [20] [21]. Although regional variation of b-value have been observed, those variations can be caused by the finite periods of earthquake catalogs, magnitude error and uncertainty of the earthquakes in the catalog, the magnitude estimation method, and the magnitude range over which the b-value is estimated. In the SHARE area source zone model, b-values are determined for the source zones with high seismicity. For the source zones with low seismicity, SHARE assumed a b-value of 1.0. For Groups 2, 3, 4 and 5, a b-value of 1.0 fits the SHARE models (Fig.3b to Fig.3e).

After α_t and β have been determined, M_c can be estimated using the seismic moment conservation principle [22]:

$$M_c \backsimeq \left[\frac{\chi \dot{M}_{T0}(1-\beta)}{\alpha_t {M_t}^{\beta} \Gamma(2-\beta)}\right]^{1/(1-\beta)} \quad (3)$$

where $\dot{M}_{T0}$ is the total tectonic moment rate determined from geodetic or geologic measurements (without considering the seismic coupling, χ), and Γ is the gamma function. The term $\chi \dot{M}_{T0}$ is equivalent to the $\dot{M}_T$ determined by Eq. (1), since the seismic coupling has been factored into the seismogenic coupled thickness, and therefore the estimation of $\dot{M}_T$. Because the uncertainties of α_t and β are much smaller than that of $\dot{M}_T$, we estimate the range of M_c simply using $\dot{M}_T \pm \sigma$. Using α_t, β, and m_c (as well as $m_c \pm \sigma$) values, we construct TGR curves for the groups (Fig.3a to Fig.3e). For Group 5, the TGR curves based on the alternative tectonic moment rate are shown in Fig.3f.

For Group 1, both the SHARE and strain-rate based models forecast higher seismicity rates than the historical catalog (Fig.3a). The strain-rate based model supports SHARE modeling higher than historical rates.

For Groups 2 and 3, the strain-rate based model and the SHARE area source zone model are fairly close (Fig.3b and Fig.3c). They are also quite consistent with the historical catalog for magnitudes below 7.0. For larger magnitudes, it is possible that events of those magnitudes were not recorded in the historical times or they were out of the catalog completeness times.

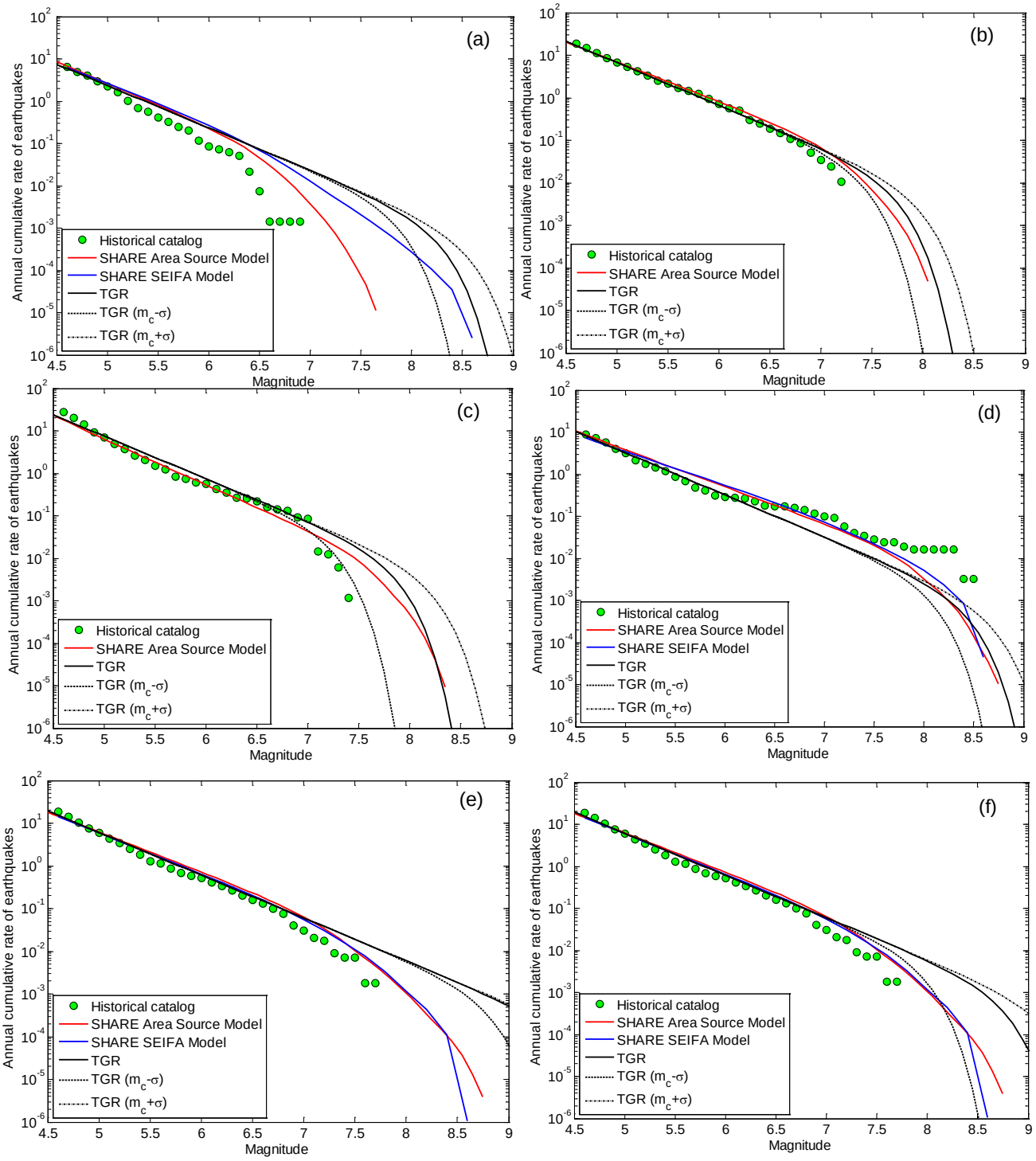

Fig. 3 - Annual cumulative rate of earthquakes for groups based on historical earthquake catalogs (green dots) and models. The TGR models are based on tectonic moment rate in Table 1. Figures (a) to (e) correspond to Groups 1 to 5, respectively. Figure (f) is also for Group 5. However, it uses the alternative tectonic moment rate for the zone, in which the Aegean megathrust surface is considered as entirely uncoupled.

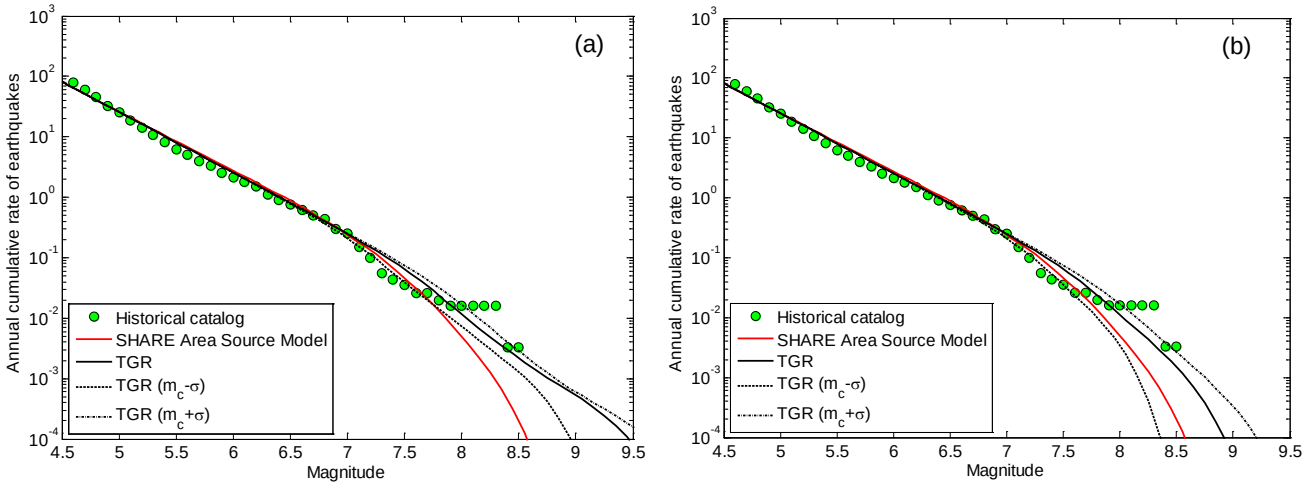

Fig. 4 - Annual cumulative rate of earthquakes for the five groups combined based on historical earthquake catalogs (green dots) and models. (b) is the same as (a) except that the TGR models for Group 5 are based on the alternative tectonic moment rate in (b).

Group 4 is the only zone in which the strain-rate based model has a lower moment rate than the SHARE models. The historical earthquake catalog shows that the apparent *b*-value is larger than 1.0 for $m_w \leq 6.5$ and smaller than 1.0 for larger magnitudes (Fig.3d). The SHARE models match the historical catalog *b*-value at large magnitudes. The strain-rate based model is closer to the historical catalog *b*-value at small magnitudes. The historical catalog includes the 1755 magnitude 8.5 Lisbon earthquake and 1941 magnitude 8.3 Azores-Cape Vincent Ridge earthquake. The Lisbon earthquake occurred in a zone in which the catalog is assumed to be complete since 1700 for $m_w \geq 6.5$. The Azores-Cape Vincent Ridge earthquake occurred in a zone in which the catalog is assumed to be complete since 1930 for $m_w \geq 5.7$. Therefore, the tail of the historical magnitude-frequency distribution is very high due to at least these two earthquakes (Fig.3d). However, the true recurrence times for such earthquakes are unknown. We suspect that the recurrence time for m_w 8.3 and larger earthquakes could be much longer than what was shown by the historical magnitude-frequency distribution. The tectonic moment rate can be a reasonable constraint for the recurrence of large earthquakes.

For Group 5, the tectonic moment rate is much higher than the seismic moment rates implied by SHARE models and historical catalogs. Thus, the TGR models forecast a much higher rate of large earthquakes than the SHARE models and historical catalogs (Fig.3e). The largest historical earthquake recorded in the group is the 1303 magnitude 8.3 Greece earthquake. The event is not shown in the historical magnitude-frequency plot because it is out of the catalog completeness time. When the alternative tectonic moment rate is used, the SHARE models are consistent with the lower bound of the TGR model (Fig.3f). Nevertheless, the SHARE models forecast a higher rate than the historical catalog for $m_w \geq 6.8$, which is supported by the strain-rate based model.

Compared to the historical earthquake data, the TGR models appear to overestimate the rate of large earthquakes except in Group 4. When the five groups are combined, the discrepancies balance out (Fig.4a). The SHARE area source model, the TGR models, and the historical earthquake data show consistent rate for magnitude as large as 7.8. Larger than m_w 7.8, the SHARE area source model shows a lower rate than the TGR models and the historical earthquake data.

Figure 4b is similar to Fig.4a except that the magnitude-frequency distribution of Group 5 is based on the alternative tectonic moment rate for the zone (Table 1), in which the Aegean megathrust surface is considered as entirely uncoupled. For this scenario, the TGR models demonstrate a lower rate at larger magnitude than the same models illustrated in Fig.4a, making the SHARE area source model more consistent with the TGR models. However, there is not enough evidence to prove which scenario is better for Group 5.

4.2 Probable maximum magnitudes of the groups

SHARE estimated m_{max} for each of the seismic sources. In doing so, SHARE adopted a statistical approach which groups source zones into superzones in order to have adequate data for a robust statistical analysis. For the regions characterized by high seismicity and in-depth knowledge of historical seismicity and seismogenic sources, SHARE relied on the maximum observed magnitude in the catalog and expected m_{max} on the faults.

The probable maximum magnitude, $m_p(T)$, defines the expected maximum magnitude within a period of time T [23]. From the magnitude-frequency distributions, we can determine $m_p(T)$ for each of the models. Table 2 lists $m_p(T)$ for 500-, 1000-, and 10,000-year time intervals for SHARE area source zone and SEIFA models and the strain-rate based model from this study. The range of $m_p(T)$ of the strain-rate based model is determined by using the lower and upper TGR curves shown in Fig.3. As a comparison, we also list the m_{max} values of the SHARE area source zone model in the table. Because each group includes area source zones with a range of m_{max} values, we only list the m_{max} values of the area source zone with the highest m_{max} in Table 2.

Table 2 – Probable maximum magnitudes expected in 500, 1000, and 10,000 years inferred from SHARE area source zone (M-AS) and SEIFA (M-SF) models, and the strain-rate based model (M-T) from this study

m_{max}-Group	m_{max}-his[£]	m_{max} of SHARE AS model[§] m_{max01} to m_{max04}				m_p(500)			m_p(1000)			m_p(10,000)		
						M-AS	M-SF	M-T	M-AS	M-SF	M-T	M-AS	M-SF	M-T
1	6.9	7.0	7.2	7.4	7.6	7.1	7.5	7.9 (7.5-8.0)	7.2	7.7	8.1 (7.8-8.2)	7.5	8.2	8.4 (8.1-8.6)
2	7.2	7.5	7.7	7.9	8.1	7.7	-	7.8 (7.6-8.0)	7.8	-	7.9 (7.7-8.1)	8	-	8.1 (7.8-8.3)
3	7.9	7.8	8.0	8.2	8.4	7.8	-	7.9 (7.5-8.2)	7.9	-	8 (7.6 -8.3)	8.2	-	8.2 (7.7-8.5)
4	8.5	8.5[#]	8.8[#]	-	-	8.1	8.2	8.1 (7.9-8.1)	8.2	8.4	8.2 (8.1-8.4)	8.5	8.5	8.6 (8.3-8.8)
5	8.3	8.2	8.4	8.6	8.8	7.9	7.9	8.4 (8.4-8.4)	8	8	8.7 (8.6-8.7)	8.4	8.4	9.5 (9.0-9.6)
5[&]	8.3	8.2	8.4	8.6	8.8	7.9	7.9	8.3 (8.0-8.4)	8	8	8.6 (8.1-8.7)	8.4	8.4	8.9 (8.3-9.2)

[£] Maximum earthquake magnitudes in the historical earthquake catalogs.

[§] The values are the m_{max} of the source zone with the highest m_{max} values within the group.

[#] Only two m_{max} values were assigned to the several area source zones from Gibraltar to Azores.

[&] The alternative scenario for Group 5, in which the Aegean megathrust surface is considered as entirely uncoupled.

For Group 1, the m_{max} values of the SHARE area source zone model are smaller than the m_p(500) of the strain-rate based model. The SEIFA model presents larger $m_p(T)$ than the area source zone model, although the values are still lower than the values inferred from the strain-rate based model. For Groups 2 and 3, the range of SHARE m_{max} and $m_p(T)$ values is compatible with the range of $m_p(T)$ values inferred from the strain-rate based model. For Group 4, SHARE m_{max} values are within the range of m_p(10,000) of the strain-rate based model. The SHARE $m_p(T)$ (T = 500, 1000, and 10,000) values are also within the range of $m_p(T)$ of the strain-rate based model. For Group 5, SHARE m_{max} values are up to 8.8. However, both the SHARE area source zone and SEIFA

model produce a magnitude of 8.4 for the period of 10,000 years. For the alternative scenario of Group 5, the SHARE m_p(10,000) values are within the range of m_p(10,000) of the strain-rate based model.

5. Discussion and Conclusions

5.1 Calculation of tectonic moment rate

We calculated tectonic moment rate from strain rate using the methods presented in [12] and [14]. We considered the uncertainties in coupled thickness of seismogenic lithosphere in the calculation of tectonic moment rates. This uncertainty contributes the most to the tectonic moment rate uncertainty, which ranges from 30% to 60% for the five groups. Additional uncertainty comes from the trade-offs in the long-term interseismic strain rates in each active cell of the GSRM v2.1 model by [4] and [5]. We compared SHARE seismic moment rates with the estimated tectonic moment rates, and we found that SHARE seismic moment rates are much lower for Groups 1 and 5, but much higher for Group 4. For Groups 2 and 3, SHARE seismic moment rates are compatible with the estimated tectonic moment rates. Ward, in [24] and [25], compared moment rates estimated from earthquake catalog and geodetic data, and found that the ratio of seismic-based and geodetic-based moment rates was 70-80% in the fastest straining regions (such as California and Italy) and reduced to 2-3% in the slowest straining regions, such as central United States and northwestern Europe. Our study area is tectonically active, which is more comparable to California.

5.2 Seismicity rate inferred from tectonic moment rate

We used TGR distributions to describe seismicity rates inferred from tectonic moment rate. For the TGR distributions, the uncertainties of the parameters α_t and β are relatively small compared to the uncertainties of the corner magnitudes (m_c). Because the uncertainty of tectonic moment rate ($\dot{M}_T$) contributes the most to the uncertainty of m_c, we calculated $m_c \pm \sigma$ using $\dot{M}_T \pm \sigma$ only. We then used $m_c \pm \sigma$ to calculate the lower and upper TGR curves. In reality, the range between lower and upper TGR curves should be somewhat broader if we consider the uncertainties of α_t and β values. Another source of uncertainty in the TGR distributions is estimating earthquake activity rates from catalogs which include magnitude errors. Tinti and Mulargia [26] showed that for magnitudes inferred directly from seismic recordings with uniform methods, random errors in magnitude generally caused a positive bias in α_t. However, Musson [27] showed that, when moment magnitudes are estimated by regression from other magnitude scales, random magnitude errors may result in underestimation or overestimation of earthquake activity rates, depending on how magnitudes are converted. In our case, it is difficult to correct the activity rates based on the SHARE catalogs because the magnitudes in the catalogs are from various sources and were converted to m_w using different regression relationships.

5.3 Conclusions

Seismicity rates are critical input for seismic hazard calculation. We used tectonic moment rates to derive seismicity rates and probable maximum magnitudes for five m_{max}-groups in southern Europe. This study showed:

1) For Group 1, the tectonic moment rate derived from GSRM v2.1 is much higher than SHARE seismic moment rates. The strain-rate based model gives even higher rates at $m_w \geq 6.5$, although SHARE models already have much higher seismicity rates than the historical rates. Compared with the probable maximum earthquake magnitudes derived from the strain-rate based model, SHARE m_{max} values are low. However, compared with the historical data, the m_{max} values used by SHARE are high.
2) For Groups 2 and 3, the differences between the tectonic moment rates and SHARE seismic moment rates are smaller than the uncertainties of the tectonic moment rates. The seismicity rates inferred from tectonic moment rates, used by SHARE models, and indicated by historical data are consistent with each other. The SHARE m_{max} values are also consistent with the probable maximum magnitudes inferred from tectonic strain rates.
3) For Group 4, SHARE seismic moment rates are higher than tectonic moment rate. The seismicity rates used by the SHARE models are higher than those inferred from the strain-rate model, but lower than those estimated from historical data. However, because SHARE used smaller *b*-values than we used for

the strain-rate based model, the m_{max} values used by SHARE are consistent with the probable maximum magnitudes expected up to 10,000 years inferred from tectonic strain rates.

4) For Group 5, the tectonic moment rate is much higher than SHARE seismic moment rates. SHARE seismicity rates are a little higher than the historical rate at large magnitudes. The strain-rate based model shows that yet higher rates are possible. The SHARE m_{max} values are consistent with the probable maximum magnitudes inferred from tectonic strain rates.
5) When the five groups are combined, the historical data, the SHARE model, and the strain-rate based model have consistent seismicity rates for magnitudes up to 7.8. For magnitudes larger than 7.8, the historical data are sparse, and the SHARE model has a lower seismicity rate than the strain-rate based model. This demonstrates that SHARE models could be more conservative.

The seismicity rates inferred from tectonic moment rates are different than the rates modeled by SHARE for Groups 1, 4, and 5 at large magnitudes. This is because the SHARE seismic source zone models and the strain-rate based model use different datasets and assumptions. The historical data are sparse for large-magnitude earthquakes and the catalog completeness times used in the calculation greatly affect the historical rates. Therefore, we cannot verify or validate the modeled seismicity rates at large magnitudes using historical earthquake data. However, the strain-rate-based model provides an alternative view of the seismicity rates and maximum earthquake magnitudes than what SHARE models present. Without this alternative view, SHARE models could only be compared with the historical data, and those comparisons show that SHARE models overestimate earthquake rates for Groups 1 and 5, and underestimate rates for Group 4. However, when we compared SHARE models with this alternative view from the strain-rate-based model, we found that SHARE models neither overestimate earthquakes rates for Groups 1 and 5, nor underestimate the rates for Group 4. In another words, the strain-rate based model supports the decision made by SHARE modelers to assign higher or lower than historical seismicity rates to some groups.

6. Acknowledgements

This work was supported by FM Global. We thank Harold Magistrale and Hosam Ali for discussions, suggestions, and for reviewing the manuscript. We also thank Franco Tamanini and Lou Gritzo for reviewing and editing the manuscript.

7. References

[1] Wössner J, Laurentiu D, Giardini D, Crowley H, Cotton F, Grünthal G, Valensise G, Arvidsson R, Basili R, Demircioglu MB, Hiemer S, Meletti C, Musson RW, Rovida AN, Sesetyan K, StucchiM, The SHARE Consortium (2015): The 2013 European Seismic Hazard Model: key components and results. *Bull. Earthquake Eng.*, **13**, 3553-3596.

[2] Giardini D, Wössner J, Danciu L (2014): Mapping Europe's seismic hazard. *EOS*, **95**(29), 216-262.

[3] Giardini D, Wössner J, Danciu L, Crowley H, Cotton F, Grünthal G, Pinho R, Valensise G, Akkar S, Arvidsson R, Basili R, Camelbeeck T, Campos-Costa A, Douglas J, Demircioglu MB, Erdik M, Fonseca J, Glavatovic B, Lindholm C, Makropoulos K, Meletti C, Musson R, Pitilakis K, Sesetyan K, Stromeyer D, Stucchi M, Rovida A (2013): Seismic Hazard Harmonization in Europe (SHARE): online data resource. doi: 10.12686/SED-00000001-SHARE.

[4] Kreemer C, Klein GE, Shen ZK, Wang M, Estey L, Wier S, Boler F (2014): Global geodetic strain rate model. *GEM Technical Report*, Pavia, Italy.

[5] Kreemer C, Blewitt G, Klein EC (2014): A geodetic plate motion and global strain rate model. *Geochemistry, Geophysics, Geosystems*, doi: 10.1002/2014GC005407.

[6] Stucchi M, Rovida A, Gomez Capera AA, Alexandre P, Camelbeeck P, Demircioglu MB, Gasperini P, Kouskouna V, Musson RMW, Radulian M, Sesetyan K, Vilanova S, Baumont D, Bungum H, Fäh D (2013): The SHARE European Earthquake Catalogue (SHEEC) 1000-1899. *J. Seismol.*, **17**, 523-544.

[7] Grünthal G, Wahlström R, Stromeyer D (2013): The SHARE European Earthquake Catalogue (SHEEC) for the time period 1900–2006 and its comparison to the European-Mediterranean Earthquake Catalogue (EMEC). *J. Seismol.*, **17**(4), 1339-1344.

[8] Grünthal G, Wahlström R (2012): The European-Mediterranean Earthquake Catalogue (EMEC) for the last millennium. *J. Seismol.*, **16**(3), 535-570.

[9] Sesetyan K, Demircioglu M, Rovida A, Albini P, Stucchi M (2013): SHARE-CET, the SHARE earthquake catalogue for Central and Eastern Turkey complementing the SHARE European Earthquake Catalogue (SHEEC). http://www.emidius.eu/SHEEC/.

[10] Bird P (2003): An updated digital model of plate boundaries. *Geochemistry, Geophysics, Geosystems*, **4**(3), 1027.

[11] Chamot-Rooke N, Rabaute A (2006): Plate tectonics from space. Commission for the Geological Map of the World, scale: 1:50000000.

[12] Bird P, Liu Z (2007): Seismic hazard inferred from tectonics: California. *Seismol. Res. Lett.*, **78**(1), 37-48.

[13] Bird P, Kagan YY (2004): Plate-tectonic analysis of shallow seismicity: Apparent boundary width, beta, corner magnitude, coupled lithosphere thickness, and coupling in seven tectonic settings, *Bull. Seism. Soc. Am.*, **94**(6), 2380-2399.

[14] Bird P, Kreemer C (2014): Revised tectonic forecast of global shallow seismicity based on version 2.1 of the Global Strain Rate Map. *Bull. Seism. Soc. Am.*, doi: 10.1785/0120140129.

[15] Howe TM, Bird P (2010): Exploratory models of long-term crustal flow and resulting seismicity across the Alpine-Aegean orogeny. *Tectonics*, **29**, TC4023.

[16] Bird P, Kagan YY, Jackson DD, Schoenberg, FP, Werner MJ (2009): Linear and nonlinear relations between relative plate velocity and seismicity. *Bull. Seism. Soc. Am.*, **99**(6), 3097-3113.

[17] Wössner J, Danciu L, Kästli P, Monelli D (2013): D6.6 - Databases of seismogenic zones, Mmax, earthquake activity rates, ground motion attenuation relations and associated logic tres. SHARE on-line documentation, http://www.share-eu.org/node/52.

[18] Kagan YY (2002): Seismic moment distribution revisited: I. Statistical results. *Geophys. J. Int.*, **148**(3), 520-541.

[19] Hanks TC, Kanamori H (1979): A moment magnitude scale. *J. Geophys. Res.*, **84**, 2348-2350.

[20] Kagan YY (1999): Universality of the seismic moment-frequency relation. *Pure Appl. Geophys.*, **155**, 537-573.

[21] Godano C, Pingue F (2000): Is the seismic moment–frequency relation universal? *Geophys. J. Int.*, **142**(1).

[22] Kagan YY (2002): Seismic moment distribution revisited: II. Moment conservation principle. *Geophys. J. Int.*, **149**(3), 731-754.

[23] Rong Y, Jackson DD, Magistrale H, Goldfinger C (2014): Magnitude limits of subduction zone earthquakes. *Bull. Seism. Soc. Am.*, **104**(5), 2359-2377.

[24] Ward SN (1998): On the consistency of earthquake moment rates, geological fault data, and space geodetic strain: the United States. *Geophys. J. Int.*, **134**, 172–186.

[25] Ward SN (1998): On the consistency of earthquake moment release and space geodetic strain rates: Europe. *Geophys. J. Int.*, **135**, 1011-1018.

[26] Tinti S, Mulargia F (1985): Effects of magnitude uncertainties on estimating the parameters in the Gutenberg-Richter frequency-magnitude law. *Bull. Seis. Soc. Am.*, **75**, 1681-1697.

[27] Musson RW (2012): The effect of magnitude uncertainty on earthquake activity rates. *Bull. Seis. Soc. Am.*, **102**(6), doi:10.1785/0120110224.